Cumhuriyet Sci. J., 44(1) (2023) 209-217
DOI: https://doi.org/10.17776/csj.1184107

Cumhuriyet Science Journal

| csj.cumhuriyet.edu.tr | Founded: 2002 ISSN: 2587-2680 e-ISSN: 2587-246X Publisher: Sivas Cumhuriyet University

Reclaim of Wrecked Bi-Te Based Materials In Peltier Modules In Thermopower Properties By Mechanical Milling

Mehmet Çetin [1,a], Gizem Durak Yüzüak [2,b], Ercüment Yüzüak [1,c,*]

[1] Department of Energy Systems, Faculty of Engineering and Architecture, Recep Tayyip Erdogan University, Rize, Türkiye.
[2] Rare Earth Elements Application and Research Center, Munzur University, Tunceli, Türkiye.
*Corresponding author

Research Article

History
Received: 04/10/2022
Accepted: 26/02/2023

ABSTRACT

We thoroughly evaluated the effects of various treatments on the structural and electrical properties of the two as-cast materials, "Sb-doping Bi-Te (p-type)" and "Se-doping Bi-Te (n-type)" which are frequently present in abandoned Peltier modules. To investigate the thermoelectric properties of Bi_2Te_3-based materials, waste alloys characterized by electrical conductivity using the hot-end method. Alloys were purified by performing arc melting on a water-cooled copper crucible in a vacuum of at least 10^{-3} mbar, with five times melting sessions to assure homogeneity. A single and long milling period of 144 hours is applied. After the compressing operation, the resulting discs with nanostructures were annealed for an hour at 600 K under vacuum conditions. The discs' structural properties were characterized using X-ray diffraction (XRD) and their surfaces and stoichiometries were determined using scanning electron microscopy with an energy dispersive feature. The Seebeck coefficient of the nanoparticle formed n-type Bi-Te based sample is -35.3 μV.K^{-1} and p-type Bi-Te based sample is 100 μV.K^{-1} (15% of mean error margin). It was found that a notable improvement was attained in comparison to the initial state with the addition of nanoparticles.

Keywords: Peltier modules, BiTe-based, Thermoelectric.

[a] mehmet_cetin21@erdogan.edu.tr https://orcid.org/0000-0001-6422-4634
[b] gizemdurakyuzuak@munzur.edu.tr https://orcid.org/0000-0002-2358-8789
[c] ercument.yuzuak@erdogan.edu.tr https://orcid.org/0000-0002-2521-9362

Introduction

Thermoelectric energy conversion (TEC) has been demonstrated as an alternate method to capture the waste heat, which is frequently situated in our environment, and convert it into electrical energy in a very cost-effective manner. TEC-based generators and derivatives have the possibility of providing an alternate option to encounter the world's energy needs and to act as a source for numerous novel ideas, such as self-generating gadgets and wearable energy technology [1, 2]. The efficiency of the material used for energy conversion is one of the most significant issues that arise in thermoelectric applications. More effective materials can be generated thanks to advancements in thermoelectric material production processes, and innovative-technologies can boost the electrical outputs and efficiencies of currently used materials. The characteristics in yield can be used to categorize energy systems lead out of thermoelectric materials, and these production parameters are influenced by the material properties used. The figure of merit (ZT), a term used to describe the performance of materials, also be used to describe these materials;

$$ZT = \frac{S^2 \sigma T}{\kappa} \quad (1)$$

where, S (μV.K^{-1}) is Seebeck coefficient, σ (S.m^{-1}) is electrical conductivity, T is temperature (K) and κ (W.K^{-1}.m^{-1}) is thermal conductivity [1]. Materials having a high Seebeck coefficient, high electrical conductivity, and low thermal conductivity are required for a good ZT output, per the equation, which we can define as the coefficient of performance.

Investigators set their sights on increasing the value of ZT from its default value of one of Eq. 1, considered a threshold. All investigations that have succeeded in increasing the performance coefficient above this amount have employed nano-structured material engineering [3]. Many novel techniques, such alloying nano systems [4], nano wires [5], and thin-film layered structures [6], have been introduced to increase material yield, and there have been extensive investigations into the progress of the thermoelectric effect and, by extension, thermoelectric materials. When Li et al. [7] exhibited a picture of the combined electrical structure and phonon mismatch in a single Sn-Se crystal system, they provided novel insight into how to attain low thermal conductivity. Equation 1 reveals that decreasing heat conductivity is an excellent strategy. However, other strategies have been developed to boost thermoelectric efficiency, including expanding the Seebeck coefficient by electronic band topologies and band changes [8] and decreasing thermal conductivity via nano-induced-configuration as thin films and/or ball-milled [9-18].

Seebeck coefficient, which allows for improvement of both the performance coefficient and the electrical output, is a highly essential parameter in the creation of improved thermoelectric materials since it yields better results with the usage of nano-sized systems. There are a variety of approaches that have been used to create materials with improved output performances. Progress was accomplished in present work by raising the Seebeck coefficient and employing a mechanical grinding mechanism to decrease large-scale thermoelectric materials to nano dimensions, resulting in an unusual shape. Mechanical grinding is employed, and the method chosen is one that can be used and maintained at minimal expense. Having been removed from an inoperable Peltier module, the thermoelectric materials that undergo grinding are considered trash. Thus, impressive outcomes have been achieved, with the potential for a Seebeck coefficient rise of up to a factor of 2. It has been demonstrated, however, that discarded thermoelectric materials may be re-evaluated and put to a good use through a variety of methods.

Degradation or damage to the thermoelectric material is a typical cause of thermoelectric module failure [19]. Temperature extremes, corrosion, and mechanical wear and tear are only some of the potential causes. In order to get non-functional thermoelectric materials back into service, it is usually required to pinpoint the root of the problem and fix it. If the thermoelectric material failed due to corrosion or oxidation, for instance, it can be salvageable by scraping off the corroded or oxidized outer layers and applying a protective coating or through an annealing procedure. It may be essential to modify the module to reduce stress on the material, or to repair or replace the damaged components, if the breakdown was brought on by thermal stress or mechanical damage. When trying to enhance the effectiveness of a thermoelectric material, it's not enough to just deal with the material-specific issues that can affect performance; the module design also needs to be optimized. By optimizing the temperature gradient across the module, heat transport can be enhanced, and parasitic losses can be minimized.

The performance and dependability of thermoelectric materials and modules have been the subject of several investigations. New materials and production methods have been the focus of recent research for thermoelectric device improvement [20, 21]. Others have studied what causes thermoelectric modules to degrade and fail, and they have provided solutions to these problems [22-24]. In conclusion, research into re-activating inactive thermoelectric materials in Peltier modules is an important topic with the potential to increase the durability and efficiency of thermoelectric devices in a variety of settings.

The purpose of bringing inoperable thermoelectric materials back into use in Peltier modules is to get them working again so they can be put to use in thermoelectric applications. Peltier modules use thermoelectric materials to create power from a temperature difference between their heated and cooled sides. However, the effectiveness of the module can diminish or be rendered useless if the thermoelectric materials deteriorate or are destroyed over time. Restoring the functioning of non-functional thermoelectric materials requires determining what caused the material's failure or degradation, then adopting solutions to fix the problems. Methods for this include cleaning the surface of the material to get rid of any impurities or corrosion, fixing or replacing any broken parts, and adjusting the module's design for better heat transfer and less stress. The purpose of putting the Peltier module back into service is not just to restore its original functionality, but to enhance its performance as well. The module's performance and its capacity to convert thermal energy into electrical energy can be enhanced by addressing the reasons that have contributed to material degradation or failure. The overall objective of re-operating inoperable thermoelectric materials in Peltier modules is to increase the lifespan of these modules and improve their performance, which can have significant implications for a variety of applications in fields like energy harvesting, cooling, and temperature sensing. This research serves as a set of answers to the question posed in the above. Separating the Peltier modules' n and p type materials allowed scientists to use the nanoparticle production process to the wasteful materials in an effort to reclaim some re-usable product.

Experimental

The electrical conductivity type was used to sort out the waste Peltier module and eliminate the Bi-Te alloys at first. The hot-end technique is used to determine if a semiconductor material is n- or p-type. A source-meter was used to assess the sort of conductivity present in the materials by measuring the voltage produced by the semiconductor when different temperatures were applied to each end.

Thermoelectric characteristics may be characterized and explored once waste Bi_2Te_3-based materials have been sorted according to conductivity classes. The arc melting technique was used to remove impurities like carbon (C) and oxygen (O) and to give a homogeneous appearance. As part of the arc melting procedure, the components were initially put in a copper crucible cooled with water before being subjected to a vacuum of up to 10^{-3} mbar and heated to melting point. This process, performed in an Edmund Bühler arc furnace, was carried out five times to provide sufficient uniformity and purity.

Initially, bulk samples were obtained; thereafter, a mechanical grinding technique was developed to conceive uniform nanostructures from Bi_2Te_3-based material. A ball mill system was constructed using steel balls, a grinding chamber, and a rotating mechanism, and grinding was performed using the planetary grinding principle with a ball-to-material ratio of 10:1 and rotation values of 150 rpm. By rotating the chamber on its own axis, centrifugal force is generated, causing the materials and balls within to move around the chamber. Due to the constant movement and wall contact of the balls, the materials in the chamber are constantly being broken down into ever-smaller increments. We used present method throughout the course of 144 hours. The nanoparticles obtained from the grinding process were annealed for 1 hour in a vacuum environment at 600 K using a Pfeiffer brand Hi-Cube vacuum station in order to avoid oxidation, decrease stress, and homogenize them. The powder was then compressed to the required particle size and pore type in an alloy pressing process. After milling the samples into a powder, they were cold pressed for an hour at 10 MPa. The procedure used to process the samples is depicted in Figure 1. Connections were built between n- and p-type materials, electrically in series and thermally in parallel, to characterize the materials' electrical properties and build a thermoelectric module.

.

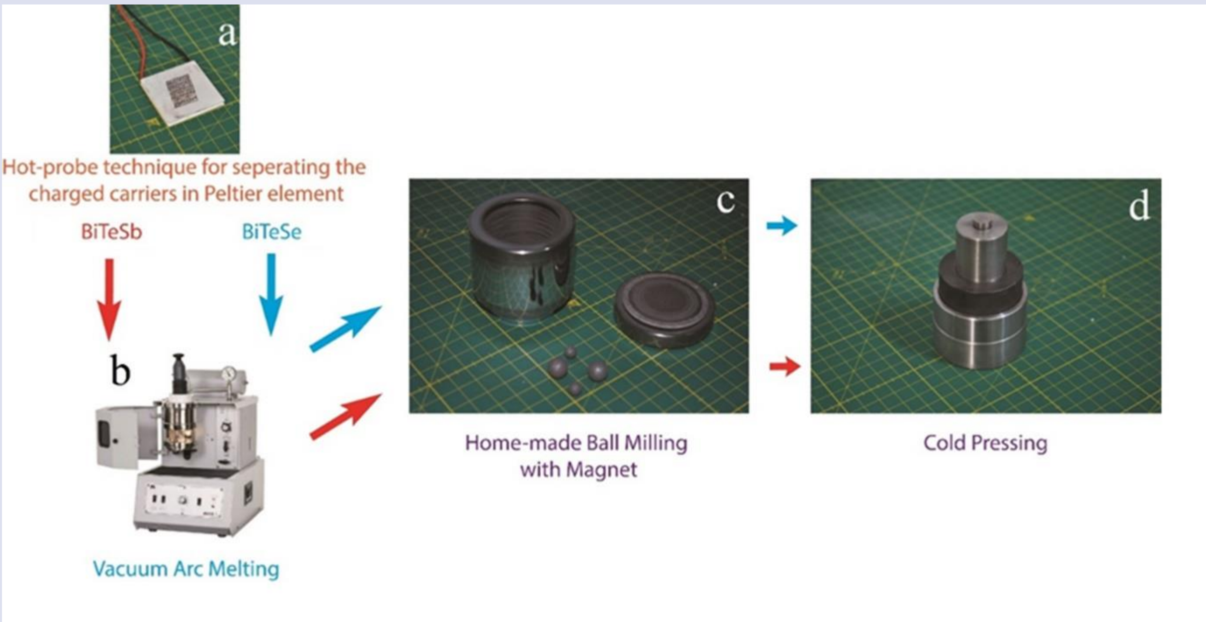

Figure 1. Processing of waste thermoelectric materials **a)** Separating n- and p-type semiconductors from the Peltier module, **b)** Preparing the samples by arc melting method, **c)** Performing the grinding process with the designed mechanical grinding system, **d)** Bringing the samples into the desired form by applying press.

Thermoelectric measurements were done after the silver paste connection was made by heating one side of the material while cooling the other. Figure 2a displays the results of the efficient and cost-effective hot-end approach used to characterize BiSbTe and BiSeTe nanoparticles (NPs). Via this method, copper wires are attached to the voltage meter's positive and negative terminals to reduce the meter's temperature rise. A distance of 1 cm must be maintained between the hot spot end of the copper wire pair and the cold end of the wire throughout the duration of the measurement to guarantee a fair comparison. A rapid increase in temperature at the probe's tip rather than the more gradual rise in temperature that would occur over a longer distance might lead to inaccurate voltage measurements. This has prompted investigations into the precise relationship between the reported voltage, the measured temperature, and the measured particle size. Instruments like the Keithley 2461 time-dependent source-meter, the Lakeshore 335 with a Si diode for temperature readings, and the Keithley 2220 electronic programmable power supply all contribute to the so-called "hot-end approach" (Figure 2b). With the use of a Keithley 2461, the difference in electrical potential between the module's two terminals was determined. A thermal imaging camera and Si-diode were used to take temperature readings from the sample's contact sites at various current levels. The error margin for the reported voltage per temperature values was 15% on average. This figure is rather close to what has been found in another research [1]. The structural and morphological features of the manufactured materials were analyzed by X-ray diffraction (XRD), scanning electron microscopy (SEM), and energy dispersive x-ray (EDX) techniques.

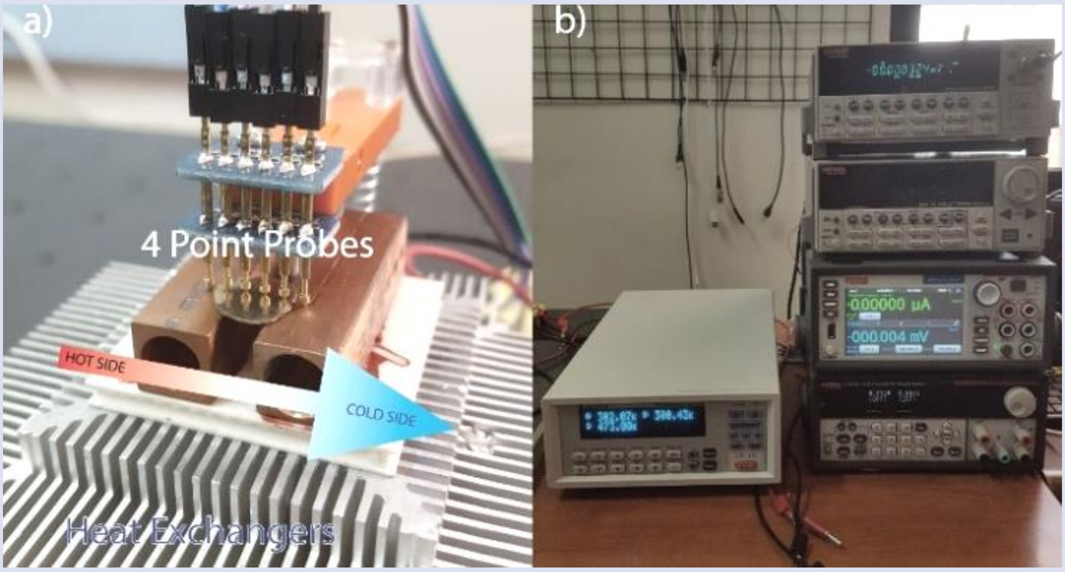

Figure 2. **a)** The hot-end measurement system designed for the characterization of the produced nanoparticles, **b)** The used devices in the study (Keithley 2461, Lakeshore 335, Keithley 2230).

Results and Discussions

X-ray diffraction analysis was used to learn more about the nanostructured discs of BiSbTe and BiSeTe that were synthesized. The as-cast and NPs' of BiSbTe and BiSeTe of XRD patterns are shown in Figures 3a and 3b, respectively. In the range of 2θ=20-110°, BiTe was identified by its diffraction peaks at 17°, 28°, 38°, 41°, 43°, 50°, 56°, and 70°. Diffraction peaks of milled alloys show the absence of several peaks ((0 0 6), (0 0 15), and (0 0 21)) that were previously present in the un-milled Sb-doping Bi-Te and Se-doping Bi-Te samples. Deformation caused by milling at room temperature is confirmed by the removal or decrease in peak intensities of reflections from basal planes. Both 2θ=26.5° and 29.5° were investigated in detail to highlight the distinctions between BiSbTe and BiSeTe in Figure 3b. It was predicted that there would be a difference of around 0.5° between the Bragg locations of the n-type and p-type materials that were produced. This scenario agrees with findings from earlier research [15, 16, 17]. Based on using the well-known Debye-Scherrer equation ($D=(k\lambda/\beta.\cos\theta)$) depicted in Figure 3b, we may infer the crystallite size and the lattice strain generated by the milling operation. Results showed that both crystal-sizes decreased without substantially altering the unit cell. Furthermore, the XRD analysis reveals that the full-with-half-maximum values of the patterns rise with essentially no change in the unit cell characteristics for both the "Sb doped" and the "Se doped" samples after the long-term low alloying technique has been applied. As a result of minimizing flaws and applying low energy to the materials over a prolonged period of time, nanoparticles have been formed. Based on the XRD data, it appears that the ball milling has a systematic effect on the crystal orientation, as seen in Figure 3b.

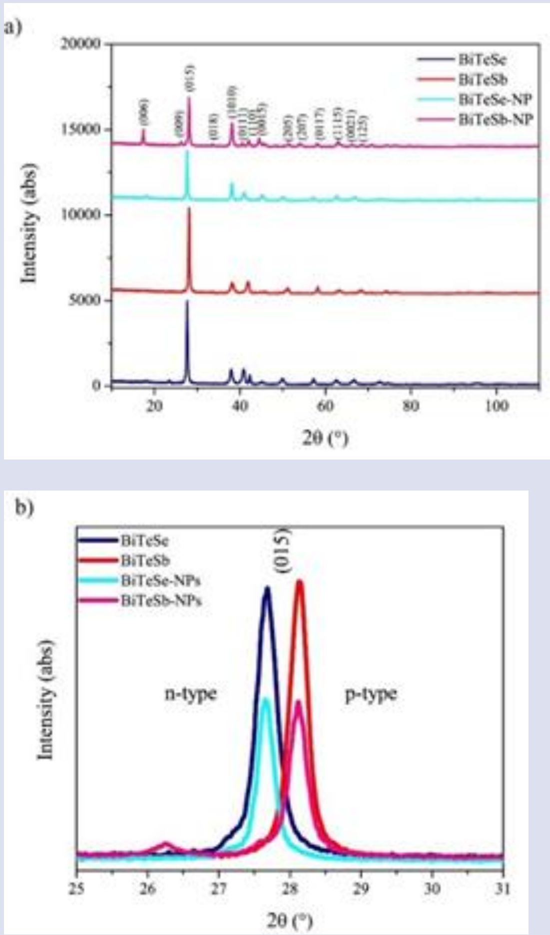

Figure 3. a) XRD patterns of as-cast and NPs' of n- and p-type BiTe alloys, and b) $(015)_{hkl}$ Bragg position of n-type and p-type materials, nanoparticles are named NPs'.

SEM was used for energy dispersive X-ray (EDX) examination to learn about the elemental composition and presence of contaminants. Figures 4a and 4b display SEM images that reveal surface information. The samples show a uniform surface roughness. The results of the EDX study may be seen in Figures 4c and 4d. It was predicted that one sample would have a high Sb content and the other a high Se content, and both predictions turned out to be true. We were able to extrapolate some information about the materials' n-type and p-type behaviors from this finding. Figures 4e and 4f also provide elemental mapping analyses, which reveal the realization of elemental distributions like Bi, Sb, Se, and Te inside the material. In order to prevent confusion, we ignore elements that make up less than 1% of the atom. The intended meaning was preserved while providing a clear interpretation.

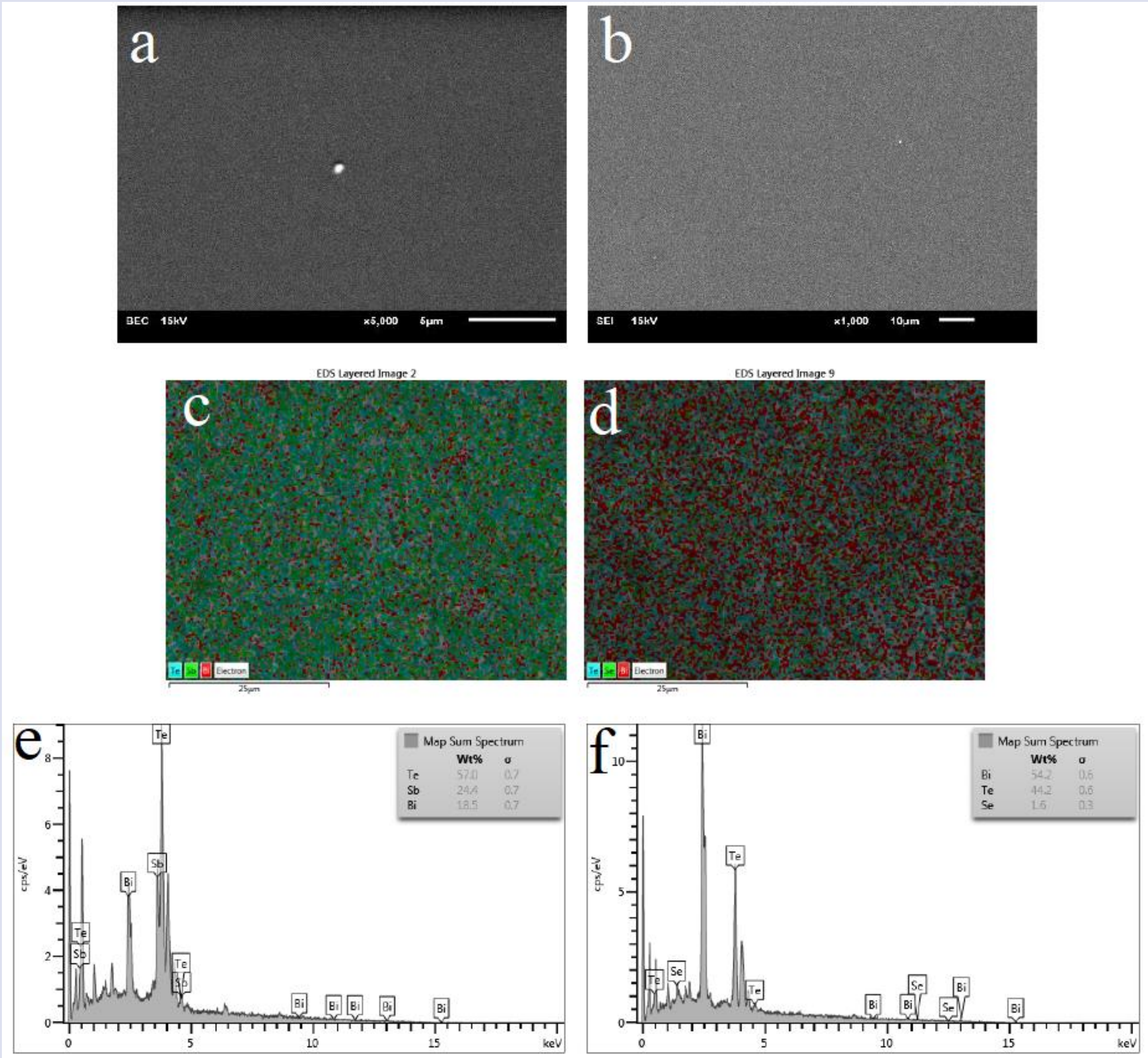

Figure 4. Structural and morphological analysis of materials, a) BiSbTe SEM image, b) BiSeTe SEM image, c) BiSbTe elemental mapping analysis, d) BiSeTe elemental mapping analysis, e) BiSbTe elemental spectrum, f) BiSeTe elemental spectrum.

Electrical measurements were taken of the materials, and the surface temperatures were measured using a thermal camera so that the Seebeck coefficients could be calculated (Figures 5a and 5b). Individual temperature calibrations and measurements were done for n and p type materials before the connections were established. Following that, it was mixed with silver paste and subjected to the aforementioned procedures again and again while still in module form. During the measurement, we subjected the heater capsule on the hot side of the manufactured module to varying currents while keeping a close eye on the temperature variations in the module's legs using a thermal imaging camera. Silver paste was used to link the legs of p-type BiSbTe and n-type BiSeTe alloys to copper wires, and the resulting resistance changes were measured.

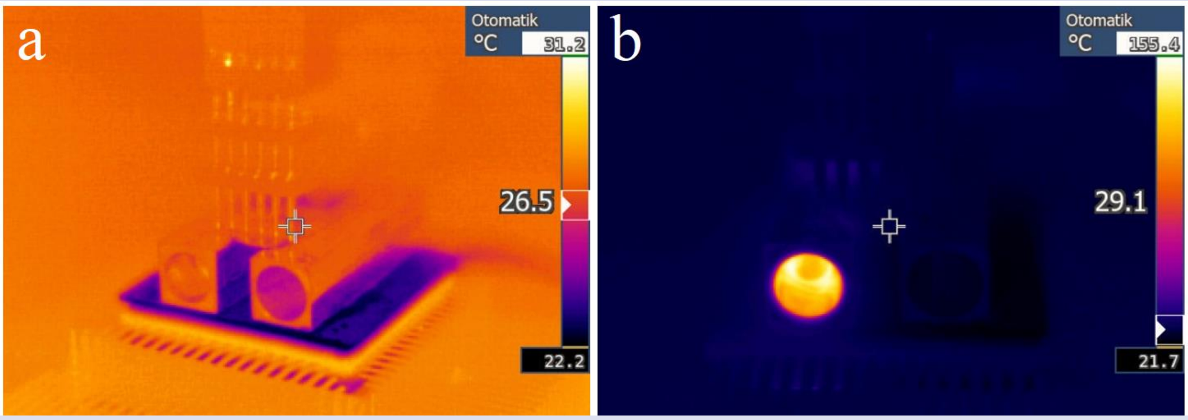

Figure 5. Thermal camera images taken from the samples, a) the temperature measured when 0 A current is applied, and b) the temperature values measured under the current of 1.4 A.

As a result, we placed in the hot tip to varying currents, ranging from minimum (0 A, as seen in Figure 5a to maximum (1.4 A), and recorded the resulting temperatures at various intervals. The maximum recorded temperature was 428 K (155°C). However, when this highest value that can be obtained brings with it some problems for the measurement system that is not in a vacuum atmosphere, in this study, the software has been developed for a programmable power supply up to a maximum current value of 0.5 A, so that the temperature difference of 22.5 K will be achieved. The thermal camera photos were taken in real time, therefore the values discovered are accurate representations of what was happening within the resistor capsule.

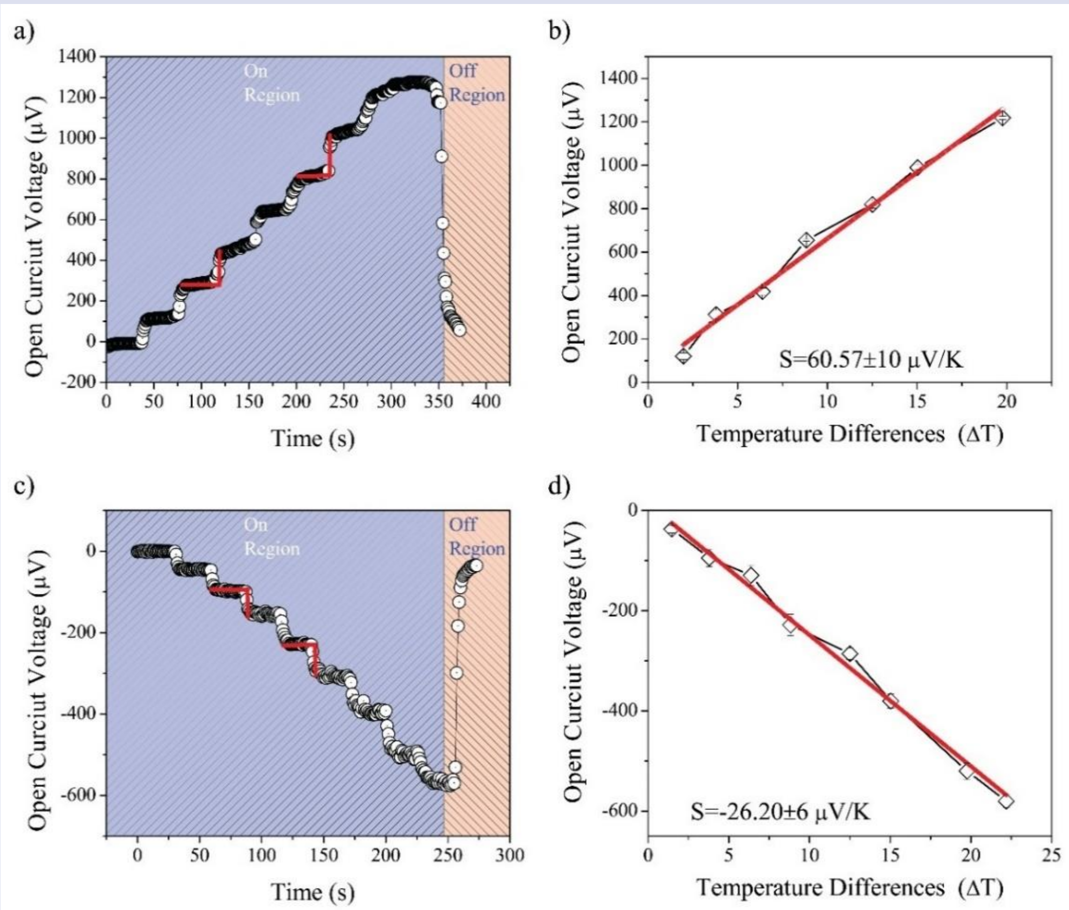

Figure 6. As-cast formed **a)** and **b)** p-type (Sb-doping), **c)** and **d)** n-type (Se-doping) materials time dependent voltage values and calculated Seebeck coefficient, respectively.

Figures 6 and 7 reveal the time- and temperature gradient-dependent electrical open circuit voltage curves of n-type and p-type materials, respectively, acquired prior to NPs' synthesis. It's easy to tell the difference between the n-type and p-type BiTe curves because of the different symmetry of the two materials. Figures 6a and 6b show the results of the Seebeck coefficient calculation using the temperature differential determined from the contact locations on the sample surface using a thermal camera. Figures 7a and 7b display the electrical values recorded following the fabrication and annealing of nanoparticles. Table 1 lists the calculated Seebeck coefficients based on these values.

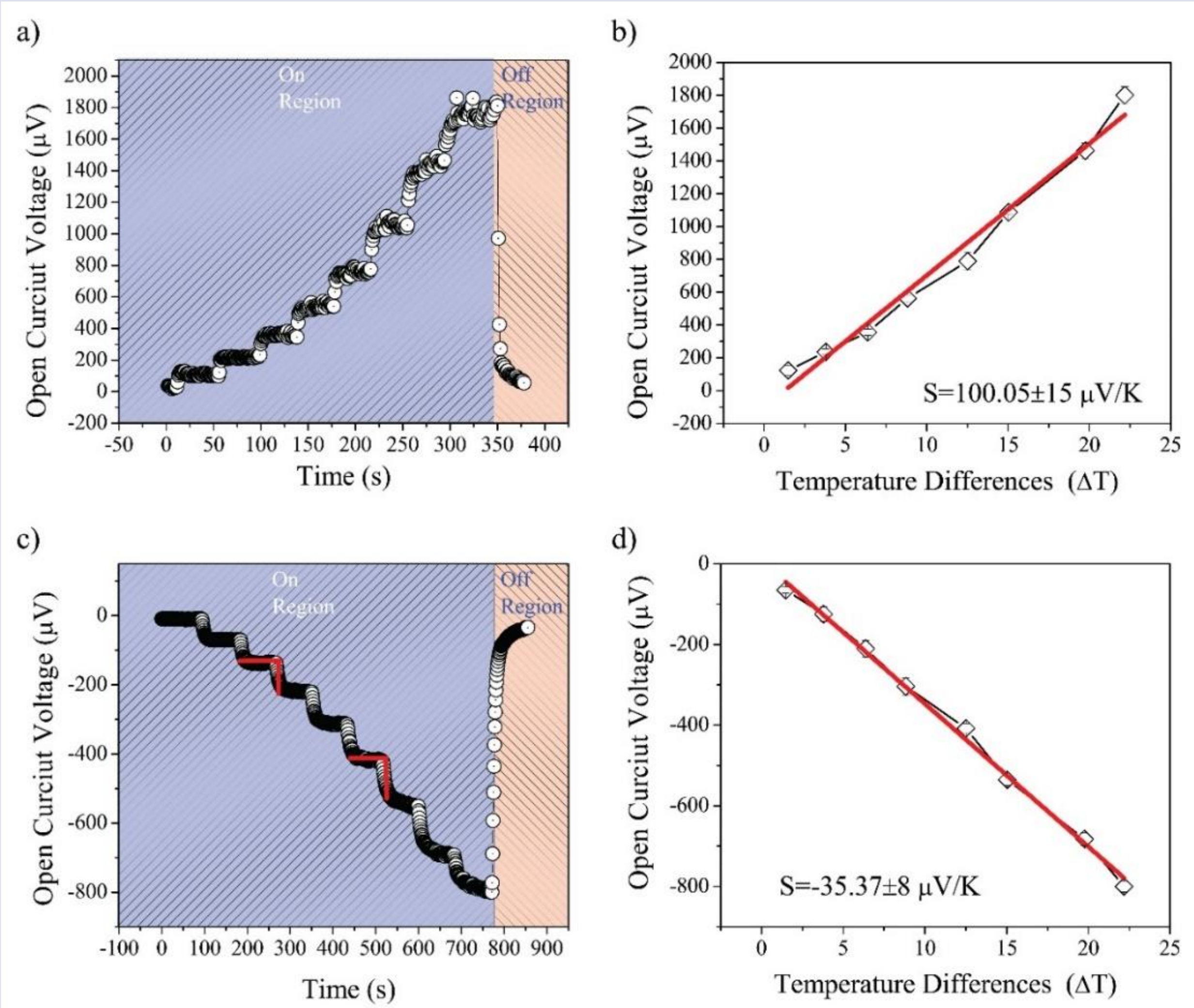

Figure 7. NPs' formed **a)** and **b)** p-type (Sb-doping), **c)** and **d)** n-type (Se-doping) materials' time dependent voltage values and calculated Seebeck coefficient, respectively.

Contrarily, there has been a lot of study done on thermoelectric materials based on thin films and milled alloys that make better use of nanostructures. Studies of thin films and milled alloys have also been substantial, and the possibility of incorporating such structures with textile goods by exploiting their adaptability has been considered [10, 11]. Table 1 provides information on the electrical outputs of a few thermoelectric materials. As can be seen in table 1, various significant advances have been made in order to increase the ZT of thin-formed and milled alloys for thermoelectric materials. The power factor improvement or the thermal conductivity reduction from microstructure engineering is the root causes of the ZT improvement.

Table 1. Electrical outputs from a selection of published nanoparticles' research

Material System	Seebeck Coefficient, S (μV/K)	Electrical Conductivity, σ (S/cm)	Electrical Resistivity, ρ (10^{-3}Ω. cm)	Thermopower (S2σ) (10^{-4} W/m. K^2)
n-Bi-Te *[11]*	-118.6	674	1,48	9,5
n-Bi-Te *[12]*	-242	360	2,77	21
n-Bi-Te *[13]*	-163	1025	0,97	27,3
n-Bi-Te *[14]*	-175	1204.3	0,83	35,2
p-Sb-Te *[14]*	155	1612.9	0,62	35,9
p-Bi-Te *[15]*	170	450	2,22	13
p-Bi-Te *[25]*	32.6	188.1	5.31	2
n-Bi-Te *[26]*	-105	1265.8	0.79	13.9
n-Bi-Te *[27]*	-172	69.9	14.3	2.07
Present Study Commercial n-Bi-Te	-26.2	1200	0.83	0.8
Present Study Commercial p-Bi-Te	60.5	900	1.11	3.2
Present Study NP n-Bi-Te	-35.3	1100	0.9	1.3
Present Study NP p-Bi-Te	100	750	1.31	7.5

Conclusions

In the present report, nanostructured Bi-Te-based alloys in defunct Peltier modules were made using conventional arc melting and a ball-milling method, and their structural, electrical, and thermal characteristics were investigated and employed to show off high-efficiency TEG modules for a heat-recovery scheme. Present advancements in this field have focused on simplifying, cheapening, and scaling up the manufacture of nanostructured materials, all in service to the creation of more effective thermoelectric devices. The following are some of the goals of this research along these lines:

Two distinct types of n-type (Se-doping) and p-type (Sb-doping) in BiTe systems were identified based on the nano-structuring used.

In order to better understand the thermoelectric effects, the argument suggests that additional study into energy harvesting from discarded gadgets is required. When the system is being subjected to temperature-induced changes, it is necessary to gain temperature dependency of thermal conductivity and Seebeck curves. If these actions are taken, it will be possible to gather valuable data that will advance the field.

Because low-speed rates inhibit the recovery and recrystallization process and encourage fracture, nanostructures with high density interfaces and defects (dislocation) can be obtained in a short amount of time by milling at low-speed rates in the nanoparticle manufacturing process (low speed - long time grinding).

The research provides more evidence that nano-structured materials can boost thermopower. As a last research recommendation, it is crucial to understand the significance of the ZT value by determining the thermal conductivity coefficient of such substances.

Acknowledgments

This work was supported by the Scientific and Technological Research Council of Turkey-TÜBİTAK, 2209-A Research Project Support Program for Undergraduate Students and it was performed at the Functional Materials Research Laboratory in Recep Tayyip Erdogan University. The authors would like to thank Sedanur Baltacı and Gaye Dülger for their helpful contributions.

Conflicts of interest

The authors declare that they have no conflict of interest.

References

[1] Shi X.-L., Zou J., and Chen Z.-G., Advanced Thermoelectric Design: From Materials and Structures to Devices, *Chemical Reviews,* 120 (2020) 7399-7515.

[2] Finn P.A., Asker C., Wan K., Bilotti E., Fenwick O., Nielsen C.B., Thermoelectric Materials: Current Status and Future Challenges, *Frontiers in Electronic Materials,* 1 (2021) 677845.

[3] Rojas J.P., Singh D., Inayat S.B., Sevilla G.A.T., Fahad H.M., Hussain M.M., Micro and nano-engineering enabled new generation of thermoelectric generator devices and applications, *ECS Journal of Solid-State Science and Technology,* 6 (3) (2017) N3036.

[4] Pan Y., Li J.F., Thermoelectric performance enhancement in n-type $Bi_2(TeSe)_3$ alloys owing to nanoscale inhomogeneity combined with a spark plasma-textured microstructure, *NPG Asia Materials,* 8 (6) (2016) e275-e275.

[5] Boukai A.I., Bunimovich Y., Tahir-Kheli J., Yu J.-K., Goddard III W.A., Heath J.R., Silicon nanowires as efficient thermoelectric materials, *Nature,* 451 (7175) (2008) 168-171.

[6] Yüzüak G.D., Çiçek M.M., Elerman Y., Yüzüak E., Enhancing the power factor of p-type BiSbTe films via deposited with/without Cr seed layer, *Journal of Alloys and Compounds*, 886 (2021) 161263.

[7] Li C.W., Hong J., May A.F., Bansal D., Chi S., Hong T., Ehlers G., Delaire O., Orbitally driven giant phonon anharmonicity in SnSe, *Nature Physics,* 11 (12) (2015) 1063-1069.

[8] Pei Y., Wang H., Snyder G.J., Band engineering of thermoelectric materials, *Advanced Materials,* 24 (46) (2012) 6125-6135.

[9] Zhao L.D., Wu H.J., Hao S.Q., Wu C.I., Zhou X.Y., Biswas K., He J.Q., Hogan T.P., Uher C., Wolverton C., Dravid V.P., Kanatzidis M.G., All-scale hierarchical thermoelectrics: MgTe in PbTe facilitates valence band convergence and suppresses bipolar thermal transport for high performance, *Energy & Environmental* Science, 6 (11) (2013) 3346-3355.

[10] Goncalves L.M., Couto C., Alpuim P., Rolo A.G., Völklein F., Correia J.H., Optimization of thermoelectric properties on Bi_2Te_3 thin films deposited by thermal co-evaporation, *Thin Solid Films,* 518 (10) (2010) 2816-2821.

[11] Nuthongkum P., Sakdanuphab R., Horprathum M., Sakulkalavek A., [Bi]:[Te] Control, Structural and Thermoelectric Properties of Flexible Bi_xTe_y Thin Films Prepared by RF Magnetron Sputtering at Different Sputtering Pressures, *Journal of Electronic Materials,* 46 (11), (2017), 6444-6450.

[12] Wang X., He H., Wang N., Miao L., Effects of annealing temperature on thermoelectric properties of Bi_2Te_3 films prepared by co-sputtering, *Applied Surface Science,* 276 (2013) 539-542.

[13] Kurokawa T., Mori R., Norimasa O., Chiba T., Eguchi R., Takashiri M., Influences of substrate types and heat treatment conditions on structural and thermoelectric properties of nanocrystalline Bi_2Te_3 thin films formed by DC magnetron sputtering, *Vacuum,* 179 (2020) 109535.

[14] Lee C.W., Kim G.H., Choi J.W., An K.-S., Kim J.-S., Kim H., Lee Y.K., Improvement of thermoelectric properties of Bi_2Te_3 and Sb_2Te_3 films grown on graphene substrate, *Physica Status Solidi (RRL)–Rapid Research Letters,* 11 (6) (2017) 1700029.

[15] Budnik A.V., Rogacheva E.I., Pinegin V.I., Sipatov A.Y., Fedorov A.G., Effect of initial bulk material composition on thermoelectric properties of Bi_2Te_3 thin films, *Journal of Electronic Materials*, 42 (7) (2013) 1324-1329.

[16] Ahiska R., Mamur H., Uliş M., Termoelektrik modülün jeneratör olarak modellenmesi ve deneysel çalışması, *Gazi Üniversitesi Mühendislik Mimarlık Fakültesi Dergisi,* 26 (4) (2011) 889-896.

[17] Hayati M., Bhuiyan M.R.A., Korkmaz F., Nil M., A review on bismuth telluride (Bi_2Te_3) nanostructure for thermoelectric applications, *Renewable and Sustainable Energy Reviews,* 82 (2018) 4159-4169.

[18] Yüzüak G.D., Özkan S., Yüzüak E., Unraveling energy consumption by using low-cost and reevaluated thermoelectric Thin Films, *Turkish Journal of Physics,* 44 (5) (2020) 442-449.

[19] Rocha Liborio Tenorio H.C., Vieira D.A., De Souza C.P., Measurement of parameters and degradation of thermoelectric modules, *IEEE Instrumentation & Measurement Magazine*, 20(2) (2017) 13-19.

[20] Zebarjadi M., Esfarjani K., Dresselhaus M.S., Ren Z.F., Chen G., Perspectives on thermoelectrics: from fundamentals to device applications, *Energy & Environmental Science*, 5 (1) (2012) 5147-5162.

[21] He J., Tritt T.M., Advances in thermoelectric materials research: Looking back and moving forward, *Science*, 357 (6358) (2017) 1-9.

[22] Shilpa M.K., Raheman M.A., Aabid A., Baig M., Veeresha R.K., Kudva N., A Systematic Review of Thermoelectric Peltier Devices: Applications and Limitations, *FDMP-Fluid Dynamics & Materials Processing,* 19 (1) (2023) 187–206.

[23] Barako M.T., Park W., Marconnet A.M., Asheghi M., Goodson K.E., Thermal Cycling, Mechanical Degradation, and the Effective Figure of Merit of a Thermoelectric Module, *Journal of Electronic Materials,* 42 (3) (2013) 372–381.

[24] Karri N.K., Mo C., Geometry optimization for structural reliability and performance of a thermoelectric generator, *SN Applied Sciences,* 1 (9) (2019) 1097.

[25] Anandan P., Omprakash M., Azhagurajan M., Arivanandhan M., Rajan Babu D., Koyama T., Hayakawa Y., Tailoring bismuth telluride nanostructures using a scalable sintering process and their thermoelectric properties, *Cryst.Eng.Comm.*, 16 (34) (2014) 7956-7962.

[26] Kim C., Kim D.H., Han Y.S., Chung J.S., Park S.H., Him H., Fabrication of bismuth telluride nanoparticles using a chemical synthetic process and their thermoelectric evaluations, *Powder technology*, 214 (3) (2011) 463-468.

[27] Zou P., Xu G., Wang S., Thermoelectric Properties of Nanocrystalline $Bi_2(Te_{1-x}Se_x)_3$ Prepared by High-Pressure Sintering, *Journal of Electronic Materials*, 44 (6) (2015) 1592-1598.